

Monitoring Disease Progression in CADASIL With Diffusion Magnetic Resonance Imaging

A Study With Whole Brain Histogram Analysis

Nicolas Molko, MD; Sabina Pappata, MD; Jean-François Mangin, PhD; Fabrice Poupon, PhD; Denis LeBihan, MD, PhD; Marie-Germaine Bousser, MD; Hugues Chabriat, MD, PhD

Background and Purpose—In cerebral autosomal dominant arteriopathy with subcortical infarcts and leukoencephalopathy (CADASIL), a large increase in water diffusion has been found both inside and outside the cerebral lesions as detected on conventional MRI. The aim of the present study was to assess the sensitivity of diffusion tensor imaging for monitoring the progression of cerebral tissue damage during the course of CADASIL.

Methods—With the use of diffusion tensor imaging, whole brain trace of the diffusion tensor [Trace(D)] histograms were obtained in 22 CADASIL patients and 12 age-matched controls at baseline, in 14 patients after a mean delay of 21 months, and in 5 controls after a mean delay of 29 months. Parameters derived from these histograms (mean value, peak height, and peak location) were analyzed at baseline and during the follow-up.

Results—At baseline, all the histogram parameters differed between patients and controls and were found to be significantly correlated with both the Mini-Mental State Examination score and Rankin Scale score in the patient group. The follow-up study showed a decrease in the peak height associated with an increase in the mean value of whole brain Trace(D) histograms in the 14 CADASIL patients scanned twice. The diffusion changes appeared larger in the patients whose Rankin score increased during the study period.

Conclusions—These results suggest that the measurement of water diffusion over time is a sensitive marker for the progression of tissue damage in the brain. Thus, quantitative diffusion MRI can be used to monitor disease progression in CADASIL and possibly in other types of small-vessel brain disorders. (*Stroke*. 2002;33:2902-2908.)

Key Words: CADASIL ■ magnetic resonance imaging

Alzheimer's disease and vascular dementia are the 2 main causes of dementia in the elderly.¹ Alzheimer's disease has been extensively investigated with MRI to obtain sensitive and specific neuroimaging markers that might be useful for preventive therapeutic strategies.^{2,3} In regard to vascular dementia secondary to small-vessel diseases, little is known concerning the natural history of the cerebral tissue lesions. This is due to the heterogeneity of the underlying vessel pathology and the frequent combination of cerebrovascular lesions with Alzheimer's disease in those older than 70 years.

Cerebral autosomal dominant arteriopathy with subcortical infarcts and leukoencephalopathy (CADASIL) has been recently identified as a new cause of "pure" vascular dementia.⁴⁻⁷ CADASIL provides a unique opportunity to investigate the pathophysiology of dementia related to small-vessel diseases for the following reasons. First, the disease is genetically homogeneous and always caused by mutations of the Notch3 gene leading to the accumulation of the 210-kDa cleavage product of the protein within the vessel wall.⁸

Second, diagnosis with genetic testing is available long before the occurrence of dementia.⁹ Third, in contrast to the specific vascular alterations, the cerebral tissue lesions in CADASIL are nonspecific and observed in various types of cerebral angiopathies.^{10,11}

One of the main characteristics of CADASIL is the presence of nonspecific white matter lesions, often termed *leukoaraiosis*, which are easily detected by T2-weighted MRI.^{12,13} As reported for other small-vessel diseases, the extent of these MRI signal abnormalities cannot predict the clinical severity.¹²⁻¹⁴ Diffusion tensor imaging is an MRI technique based on the measurement of water diffusion, which is due to the random motion of water molecules resulting from thermal energy.¹⁵⁻¹⁷ During these diffusion-driven displacements, water molecules interact with many tissue components such as cell membranes, nerve fibers, and macromolecules, which provides unique clues to the tissue structure at a microscopic level. The exquisite sensitivity of diffusion tensor imaging to tissue microstructure has been

Received February 8, 2002; final revision received June 25, 2002; accepted July 8, 2002.

From INSERM U562 (N.M., S.P.) and UNAF (J-F.M., F.P., D.L., M-G.B., H.C.), IFR 49, SHFJ-CEA, Orsay, and Department of Neurology, CHU Lariboisière (H.C.), Paris, France.

Reprint requests to Pr Hugues Chabriat, Service de Neurologie, CHU Lariboisière, 2 rue Ambroise Paré, 75010 Paris, France. E-mail hugues.chabriat@lrb.ap-hop-paris.fr

© 2002 American Heart Association, Inc.

Stroke is available at <http://www.strokeaha.org>

DOI: 10.1161/01.STR.0000041681.25514.22

TABLE 1. Main Characteristics of CADASIL Patients Included in the Longitudinal Study at Baseline and Over the Follow-Up

Age	M/F	Mutation (exon/position)	RankinScore			Interval Between MRI 1 and 2, mo	Interval Between MRI 2 and 3, mo	New Clinical Events (strokes)
			At MRI 1	At MRI 2	At MRI 3			
58	M	4/475	1	1	2	23	14	1 transient and 1 completed
64	M	3/406	1	1	1	24	13	...
66	F	3/406	3	3	4	24	14	...
66	M	23/1261	5	5	...	27
63	M	4/622	1	2	...	44
43	M	4/622	1	1	...	23
58	M	4/622	1	1	...	29
67	F	23/3859	5	5	...	25
54	F	18/3031	1	1	1	20	16	...
65	M	4/del 419-439	3	3	...	20	...	1 transient
48	M	4/499	2	2	3	12	14	...
60	M	3/406	1	2	2	12	14	1 completed
48	F	4/622	1	1	1	12	13	1 transient
44	M	4/631	1	1	...	18

used to reveal subtle tissue modifications in various diseases such as multiple sclerosis,¹⁸ Alzheimer's disease,¹⁹ schizophrenia,²⁰ and dyslexia.²¹ In CADASIL, a large increase in water diffusion has been reported within the white matter²² and basal ganglia²³ both inside and outside the cerebral lesions as detected with conventional MRI. This increase in molecular water displacement is presumably related to the enlargement of the extracellular space caused by demyelination and axon loss and is strongly correlated with cognitive and motor disabilities.

The aim of the present cross-sectional and longitudinal study was to determine differences in diffusion at baseline between patients and controls and to assess the sensitivity of diffusion tensor imaging for monitoring the progression of cerebral tissue damage during the course of CADASIL.

Subjects and Methods

Subjects

Twenty-two CADASIL patients from 10 unrelated families and with deleterious mutations of the Notch3 gene were selected (mean age, 54±11 years). All subjects underwent a first MRI study (MRI 1). Of these patients, 14 patients (mean age, 57±8 years) were included in the follow-up study and evaluated by a second MRI (MRI 2) within 1 or 2 years (mean delay from MRI 1 to MRI 2=21±6 months) (Table 1). Seven patients (mean age, 56±7 years) agreed to undergo a third MRI study (MRI 3) (mean delay from MRI 2 to MRI 3=14±1 months).

Twelve healthy subjects (mean age, 51±11 years) were selected on the basis of the following criteria: (1) no familial vascular disorder; (2) no history of neurological disorder; (3) normal neurological and general examinations; (4) Mini-Mental State Examination (MMSE) score >28; and (5) normal T1- and T2-weighted MRI. Five subjects (mean age, 44±14 years) had a second MRI study within a period of approximately 2 years (mean delay=29±6 months).

All subjects had a detailed standard neurological examination at the time of each MRI study. The global cognitive status was evaluated with the MMSE^{24,25} and the *Diagnostic and Statistical Manual of Mental Disorders, Fourth Edition (DSM-IV)* criteria²⁶ for diagnosis of dementia. The degree of physical disability was evalu-

ated with the Rankin Scale score (5-item scale from 1 [no significant disability] to 5 [severe disability]).^{27,28}

Informed consent was obtained from each participant. An independent institutional ethical committee approved the protocol used in this study (CCPPRB Kremlin-Bicêtre 9724).

Magnetic Resonance Imaging

T1- and diffusion-weighted images were acquired with the use of a 1.5-T MRI system (Signa General Electric Medical Systems) equipped with gradient hardware allowing up to 22 mT/m, which was regularly monitored for quality assurance. A standard quadrature head coil was used for radiofrequency transmission and reception of the MR signal. Reduction of head motion was achieved with the use of standard foam padding as provided by the manufacturer.

T1-weighted images were acquired first in the axial plane with the use of a spoiled gradient echo sequence (124 slices 1.2 mm thick, repetition time=10.3 ms, echo time=2.1 ms, inversion time=600 ms) and 24×24-cm field of view (resolution of 0.937×0.937×1.2 mm). Acquisition time was 7 minutes 38 seconds.

Diffusion-weighted images were acquired with echo-planar imaging in the axial plane at 26 slice locations, 5 mm thick. For each slice location, a T2-weighted image with no diffusion sensitization (b_0), followed by 11 b values (increasing linearly to a maximum value of 1000 s/mm²), was obtained in 6 noncolinear directions. The total acquisition time for diffusion tensor imaging was 8 minutes 12 seconds.

Image Postprocessing

Before the tensor estimation was performed, an unwrapping algorithm was applied to the diffusion-weighted data set to correct for distortions related to eddy currents induced by the large diffusion-sensitizing gradients.²⁹ After this correction, the diffusion tensor parameters were calculated on a pixel-by-pixel basis, and the trace of the diffusion tensor, Trace(D), was calculated as described by Bassler et al.³⁰

In all subjects, a single examiner, blind to the patient's clinical status, delineated a mask of the cerebral tissue on each slice of Trace(D) images using semiautomated software dedicated to segmentation. This software was based on a regional growing algorithm and local thresholding. The total volume of cerebral tissue (including all visible lesions) was obtained after exclusion of the surrounding extracerebral tissue and cerebrospinal fluid. The mask used to determine the whole brain volume was then checked visually for

accuracy on both b_0 and Trace(D) images, and, when necessary, corrections were made with computer-aided drawing tools. We then computed the histogram of Trace(D) for each subject using a bin width equal to $0.08 \times 10^{-3} \text{ mm}^2/\text{s}$ for the axis and a fixed upper limit of $8 \times 10^{-3} \text{ mm}^2/\text{s}$. To correct for cross-subject differences in brain volume, each histogram was normalized to the total number of voxels corresponding to the brain tissue. For each histogram, the following parameters were derived: the peak height, ie, the fraction of pixels at the most common value, and the peak location, ie, the most common value and the mean value. The time required to obtain whole brain Trace(D) histogram varied from 20 to 30 minutes for each patient. The reliability of the segmentation procedure was evaluated in 7 randomly selected subjects by 2 raters. The mean interrater and intrarater coefficient of variation of the number of voxels selected by this procedure was <1% (0.4% and 0.9%, respectively). The interrater and intrarater variability values calculated for the histogram parameters were 0.5% and 0.4% for the mean value, 0.8% and 0.7% for the peak height, and 0.03% and 0.03% for the peak location, respectively.

Statistical Analysis

The diffusion parameters obtained at MRI 1 were first compared among patients ($n=22$) and controls ($n=12$) with a 2-tailed Student's t test. Afterward, we analyzed the diffusion parameters obtained in the group of subjects included in the follow-up study (patients, $n=14$; controls, $n=5$) using a 2-way ANOVA with 2 fixed factors (group: patients and controls; time: MRI 1 and MRI 2) assuming repeated measurements and a possible time-group interaction. For post hoc analysis, a t test with Bonferroni correction was applied to compare group means. In the subgroup of patients with 3 repeated examinations, the variations of diffusion parameters between each MRI were analyzed with a paired t test. The effects of diffusion parameters at baseline, the interexamination delay, and age were tested by multiple regression analysis. The Spearman rank test was used to assess correlation between diffusion parameters and the clinical scores, and the Friedman test was used to analyze changes in clinical scores between the 3 MRI studies.

Values of $P < 0.05$ were considered statistically significant. The statistical analysis was performed with the use of Statview software (Abacus Concepts Inc).

Results

Clinical Data

Twenty patients had the typical clinical manifestations of CADASIL, and 2 were asymptomatic. Eight had a history of recurrent attacks of migraine with aura; 14 had previous transient ischemic attacks and/or completed strokes, with a permanent focal deficit in 8 patients. Six were demented, and 7 had a Rankin Scale score >2 .

Five new ischemic events (3 transient and 2 completed) occurred in 4 patients during the follow-up (Table 1).

The average MMSE and Rankin scores obtained at the first scan in the whole group (22 patients) were 25.3 ± 7.8 and 1.95 ± 1.35 , respectively. For the group of patients ($n=14$) who had both first and second MRI scans, no significant change of the average MMSE or Rankin scores was observed between the 2 examinations. For the subgroup of patients ($n=7$) who had first, second, and third MRI scans, we also did not observe any significant change between the first and second scans. In this subgroup, the Rankin score was significantly increased at the time of the third scan (median values: 1 [range, 1 to 3] versus 2 [range, 1 to 4]; $P=0.03$), while the MMSE score remained unchanged.

MRI Study

In controls, the values of Trace(D) fell within a small range. The averaged whole brain Trace(D) histogram was characterized by a narrow peak (Figure 1A), and the coefficients of variation of histogram parameters were low (2.6%, 5.0%, and 3.6% for the mean, peak height, and location values, respectively).

In CADASIL patients, the average whole brain Trace(D) histogram was also unimodal but had wider distribution (Figure 1A). The peak height was significantly lower (7.3% versus 11.1%; $P < 0.0001$) and shifted toward higher diffusion values (2.43 versus $2.22 \times 10^{-3} \text{ mm}^2/\text{s}$). The mean value of Trace(D) measured over the whole brain was significantly higher in patients than in controls (2.82 ± 0.27 versus $2.43 \pm 0.06 \times 10^{-3} \text{ mm}^2/\text{s}$; $P < 0.0001$). ANOVA for subjects included in the follow-up study confirmed the difference between patients and controls for the mean value, peak height, and location of Trace(D) histograms (Table 2) and showed a significant time effect. An increase in the mean Trace(D) value and a decrease in the peak height of Trace(D) histograms were observed in patients, while no change was found in the control group (Table 2 and Figure 1B).

In the subgroup of 7 patients who underwent a third MRI, significant changes in the histogram parameters between MRI 1 and MRI 2 were also observed (mean value, 2.74 ± 0.18 versus $2.80 \pm 0.2 \times 10^{-3} \text{ mm}^2/\text{s}$ [$P=0.04$]; peak height, 0.80 ± 0.20 versus 0.73 ± 0.20 [$P=0.01$]). Moreover, a further increase in the mean value and a decrease in the peak height of Trace(D) histograms were found between MRI 2 and MRI 3 (MRI 3, mean value, $2.97 \pm 0.29 \times 10^{-3} \text{ mm}^2/\text{s}$ [$P=0.001$]; peak height, 0.65 ± 0.02 [$P=0.006$]) (Figure 1C).

Multiple regression analysis showed that the degree of changes (absolute values) in the mean value of Trace(D) found in patients between MRI 1 and MRI 2 was strongly correlated with the mean value of Trace (D) at baseline ($n=14$ patients; $r=0.63$, $P=0.01$). This effect was independent of age and interscan delay. The individual mean values of Trace(D) histograms are presented in Figure 2. The larger variations of this parameter are observed in patients with high diffusion values measured at baseline. Visual analysis of Trace(D) maps in a CADASIL patient illustrates these results (Figure 3). The increase in diffusion over time in this patient does not appear restricted to a focal area and predominates within the already affected regions.

Clinical Correlates

In the whole group of patients ($n=22$), the MMSE scores at the time of the first scan were positively correlated with the peak height and negatively correlated with both the mean value and the peak location of Trace(D) histograms. Conversely, the Rankin scores were negatively correlated with the peak height and positively correlated with both the mean value and peak location of Trace(D) histograms (Table 3 and Figure 4). In the subgroup of 14 patients, these correlations remained significant at both the first and second scan times.

On an individual level, the Rankin score increased in 5 patients (+1 point in each patient) during the interval of the MRI studies (Table 1). In these patients, the increase in the mean value of Trace(D) measured between the first and the last scan

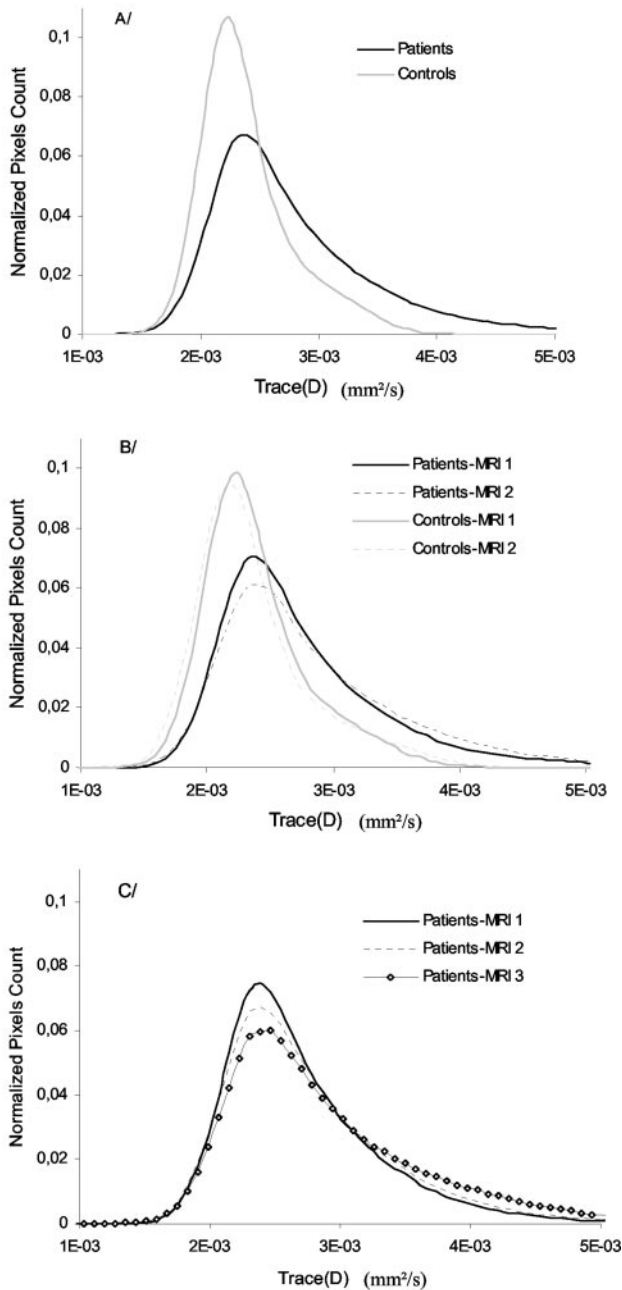


Figure 1. Average Trace(D) histograms in controls (n=12) and patients (n=22) at baseline (A). Compared with controls, the peak of the average histogram in patients shows a shift toward higher diffusion value associated with the lowering of its height. Average Trace(D) histograms were obtained in 14 patients investigated twice (B) and in the subgroup of 7 patients investigated 3 times (C). A significant increase in the mean value associated with a decrease in the peak height was observed between MRI 1 and MRI 2 in patients (mean delay=21±6 months). In the subgroup of patients investigated 3 times, an increase in the mean value associated with a decrease in the peak height was observed both between MRI 1 and MRI 2 (mean delay=18±5 months) and between MRI 2 and MRI 3 (mean delay=14±1 months).

was significantly higher than that observed in the patients whose Rankin score was unchanged (0.304 ± 0.012 versus $0.107 \pm 0.004 \times 10^{-3} \text{ mm}^2/\text{s}$; $P=0.002$) in the absence of significant difference for the interscan delay (34 ± 8 versus 27 ± 8 months; $P=0.1$).

TABLE 2. Histogram Parameters in Patients and Controls at Baseline and During the Follow-Up Study

	Patients	Controls
Baseline	n=22	n=12
Mean value ($10^{-3} \text{ mm}^2/\text{s}$)	$2.82 \pm 0.27^*$	2.44 ± 0.06
Peak height, %	$7.3 \pm 2.1^*$	11.1 ± 0.9
Peak location ($10^{-3} \text{ mm}^2/\text{s}$)	$2.43 \pm 0.15^*$	2.22 ± 0.08
Follow-up	n=14	n=5
Mean value ($10^{-3} \text{ mm}^2/\text{s}$)		
MRI 1	$2.80 \pm 0.25 \dagger$	2.44 ± 0.05
MRI 2	$2.91 \pm 0.06 \dagger \ddagger$	2.41 ± 0.09
Peak height, %		
MRI 1	$7.6 \pm 2.0 \dagger$	10.0 ± 1.4
MRI 2	$6.6 \pm 2.0 \dagger \ddagger$	9.9 ± 0.4
Peak location ($10^{-3} \text{ mm}^2/\text{s}$)		
MRI 1	$2.43 \pm 0.15 \dagger$	2.23 ± 0.05
MRI 2	$2.47 \pm 0.19 \dagger$	2.17 ± 0.10

* $P < 0.0001$, patients vs controls.

† $P < 0.01$, patients vs controls.

‡ $P < 0.01$, MRI 1 vs MRI 2 (enduring Bonferroni correction).

Discussion

This is the first imaging study to quantitatively monitor the progression of cerebral tissue damage during the course of CADASIL with the use of whole brain Trace(D) histograms. Our results show that the measurement of water diffusion is a sensitive marker of the microstructural tissue loss occurring within the brain during the course of this disease. Previous diffusion tensor imaging studies in CADASIL were performed with the use of regions of interest that provide a local estimate of microscopic tissue damage within the brain. With this method, a significant increase in Trace(D) and a decrease in anisotropy were previously reported within both the abnormal and normal-appearing white matter, as observed on conventional MRI.²² Recently, early modifications of diffusion have been detected in the normal-appearing subcortical gray matter in CADASIL patients.²³ Together, these data indicate that the cerebral tissue damage in CADASIL is much more widespread than is evident after conventional MRI. We

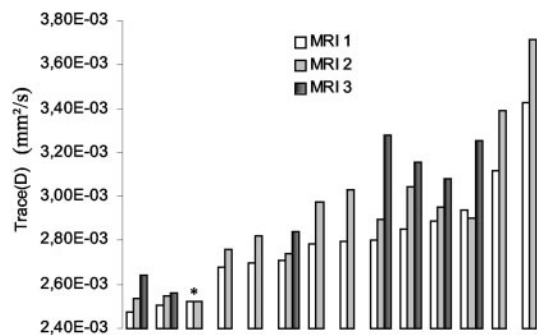


Figure 2. Individual mean values of Trace(D) histograms in patients. The data were classified in ascending order according to the mean value calculated at baseline. Note that the increase in the mean value of Trace(D) appears larger in patients with high diffusion values at baseline. In contrast, no change was detected in the only asymptomatic patient (star).

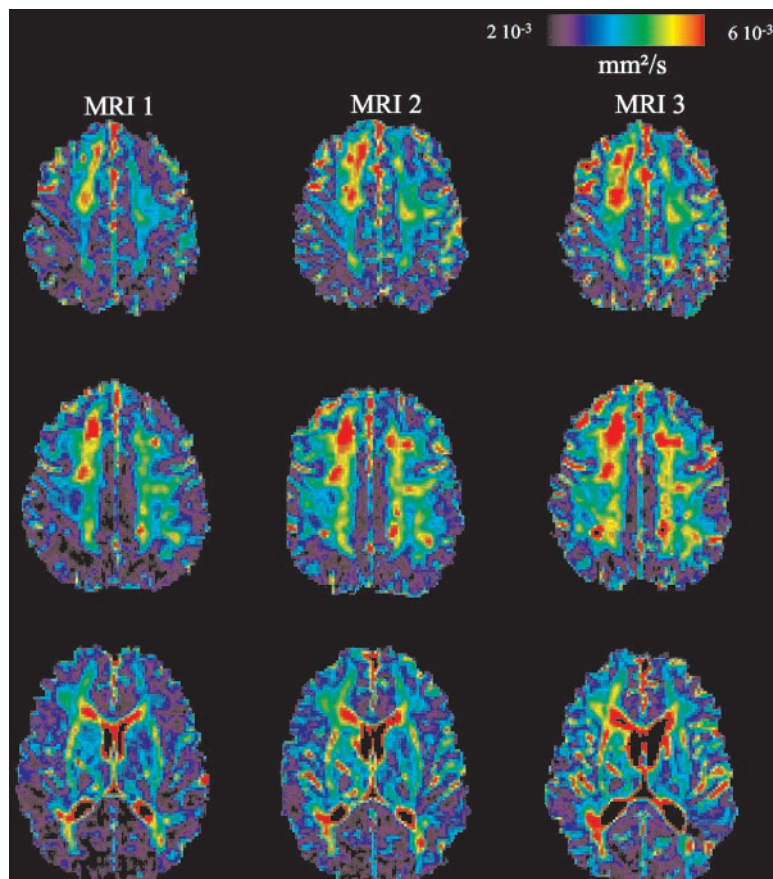


Figure 3. Diffusion images illustrating the diffusion increases in a CADASIL patient occurring over 3 years. These images show that the diffusion modifications observed are not restricted to a few voxels within a single region but are diffuse and mainly involve tissue that is already affected.

thought that the local measurement of diffusion was not relevant to monitor the progression of tissue damage in such a diffuse condition. Thus, to assess the overall burden of cerebral lesions, we selected a global approach with whole brain Trace(D) histogram analysis. This approach, already used in multiple sclerosis patients,³¹ combines the sensitivity of diffusion tensor imaging to assess both macroscopic and microscopic tissue damage with the ability to obtain a complete measurement of diffusion throughout all the voxels containing cerebral tissue. In contrast to techniques based on regions of interest, this approach cannot provide any information concerning the regional pattern of tissue changes. However, the whole brain histogram analysis is highly reproducible^{32,33} and provides easily comparable data for longitudinal studies without any image registration or subjective delineation of anatomic regions.

In healthy subjects, Trace(D) histograms are characterized by a unimodal distribution with a narrow peak, indicating that most of the diffusion values measured in the cerebral volume

are contained within a small range. In CADASIL patients, Trace(D) histograms are also characterized by a unimodal distribution. However, in contrast to controls, the peak height is reduced and shifted toward higher diffusion values with a significant increase in the mean value of Trace(D). Together, these changes indicate that diffusion is increased in most of the cerebral voxels in CADASIL patients. The main parameters derived from Trace(D) histograms were also highly

TABLE 3. Correlations Between the Parameters Derived From Trace(D) Histograms and the Clinical Scores in the Whole Group of Patients at Baseline (n=22)

	MMSE Score (<i>r</i>)	<i>P</i>	Rankin Score (<i>r</i>)	<i>P</i>
Mean value	-0.677	0.002	0.754	<0.001
Peak height	0.653	0.003	-0.533	<0.001
Peak location	-0.670	0.004	0.674	0.002

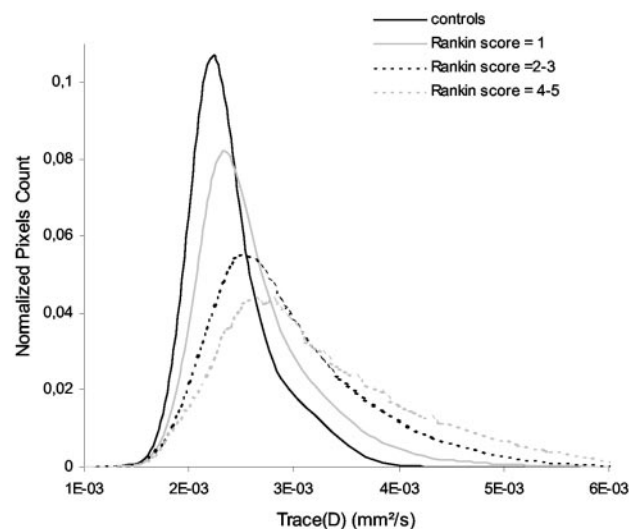


Figure 4. Averaged Trace(D) histograms in patients (n=22) at baseline according to Rankin score.

variable in our patients, which suggests different degrees of tissue changes in symptomatic patients, as previously observed with other MRI methods.³⁴ Finally, our data show that the main parameters derived from baseline Trace(D) histograms are strongly correlated with both the Rankin and MMSE scores in our patients. These results further support the idea that the clinical phenotype in CADASIL is closely related to a global measure of the amount and severity of microstructural tissue changes at the cerebral level.^{22,23} They also establish the clinical value of parameters derived from whole brain Trace(D) histograms in CADASIL.

During the follow-up study performed in 14 patients, significant modifications of Trace(D) histograms were observed after a mean delay of 21 months. The increase in the mean value and decrease in the peak height of Trace(D) histograms detected during this period indicate that the number of voxels with high diffusion values had increased in the patient group. These changes were detected in the absence of significant change of global clinical scales. These data suggest that global histogram analysis of diffusion tensor imaging is highly sensitive for detecting the disease progression in CADASIL. Interestingly, the data obtained in the subgroup of 7 patients who underwent 3 MRI exams show that diffusion further increased between MRI 2 and MRI 3, which suggests that significant modifications of Trace(D) histograms can be detected in a period as short as 14 months. Finally, at the end of the follow-up study, modifications of the Rankin score were noted in 5 patients whose increase in diffusion was greater than that measured in patients with a stable clinical status. Because of the limited size of our sample and the large variability of interscan intervals, this result should be interpreted with caution. Other studies are necessary to further investigate the relationships between the increase in diffusion over time and the clinical worsening in CADASIL.

These results provide new insights into the pathophysiology of CADASIL. It is noteworthy that diffusion changes in the cerebral tissue were detected in our series, even though only 2 new completed ischemic strokes occurred during the follow-up period. This suggests that the microstructural alterations underlying the diffusion changes can progress in the absence of acute ischemic events. In addition, these microstructural alterations appear widespread enough to be detected through a global analysis over the whole brain. The positive correlation between the baseline mean Trace(D) value and the degree of diffusion increase over time suggests that the amount of microstructural damage might influence the progression of tissue loss during the course of CADASIL. It is noteworthy that the only asymptomatic patient included in our follow-up study, who had a very low burden of lesions, was also the only person to have unchanged parameters of the Trace(D) histogram over the period of the study. Conversely, the visual examination of Trace(D) maps in symptomatic patients shows that the increase in diffusion during the course of the disease predominates within the affected cerebral areas. This might be related either to the growth of secondary degenerative processes occurring after the accumulation of ischemic lesions or to progressive tissue damage caused

directly by chronic ischemia.²³ Further investigations are necessary to settle this issue.

The present diffusion tensor imaging study shows that water diffusion progressively increases over time in the cerebral tissue during the course of CADASIL and that these diffusion changes precede the clinical worsening of CADASIL patients. To date, no therapeutic trial has been performed in CADASIL patients. Such a trial is particularly difficult to design because of the rarity of the disease, the variability of the symptoms, and the long course of the disease over several decades. The present study provides preliminary data suggesting that diffusion tensor imaging is a sensitive measure for monitoring tissue changes over a relatively short period of time and could thus be used in future therapeutic trials in CADASIL. Whether this approach is useful for monitoring disease progression in other types of small-artery disease requires further investigation.

Acknowledgments

The applications of diffusion imaging in CADASIL was supported by a grant from Assistance Publique des Hôpitaux de Paris (PHRC96-AOM96084). Genetic studies were performed by Professor E. Tournier-Lasserre and Dr A. Joutel at INSERM U25. We are grateful to all the patients and their families who participated in this study.

References

1. Desmond DW. Vascular dementia: a construct in evolution. *Cerebrovasc Brain Metab Rev.* 1996;8:296–325.
2. Fox NC, Crum WR, Schill RI, Stevens JM, Janssen JC, Rossor MN. Imaging of onset and progression of Alzheimer's disease with voxel-compression mapping of serial magnetic resonance images. *Lancet.* 2001;358:201–205.
3. Adalsteinsson E, Sullivan EV, Kleinmans N, Spielman DM, Pfefferbaum A. Longitudinal decline of the neuronal marker N-acetyl aspartate in Alzheimer's disease. *Lancet.* 2000;355:1696–1697.
4. Joutel A, Corpechot C, Ducros A, Vahedi K, Chabriat H, Mouton P, Alamowitch S, Domenga V, Cecillion M, Marechal E, Maciazek J, Vayssiere C, Cruaud C, Cabanis EA, Ruchoux MM, Weissenbach J, Bach JF, Bousser MG, Tournier-Lasserre E. Notch3 mutations in CADASIL, a hereditary adult-onset condition causing stroke and dementia. *Nature.* 1996;383:707–710.
5. Chabriat H, Vahedi K, Iba-Zizen MT, Joutel A, Nibbio A, Nagy TG, Krebs MO, Julien J, Dubois B, Ducrocq X, Levasseur M, Homeyer M, Mas JL, Lyon-Caen O, Tournier-Lasserre E, Bousser MG. Clinical spectrum of CADASIL: a study of 7 families: cerebral autosomal dominant arteriopathy with subcortical infarcts and leukoencephalopathy. *Lancet.* 1995;346:934–939.
6. Chabriat H, Bousser M. Pure vascular dementia. In: Leys D, Pasquier F, Scheltens P, eds. *Stroke and Alzheimer's Disease.* The Hague, Netherlands: Holland Academic Graphics; 1999:28–43.
7. Dichgans M, Mayer M, Uttner I, Bruning R, Muller-Hockner J, Rungger G, Ebke M, Klockgether T, Gasser T. The phenotypic spectrum of CADASIL: clinical findings in 102 cases. *Ann Neurol.* 1998;44:731–739.
8. Joutel A, Andreux F, Gaulis S, Domenga V, Cecillion M, Battail N, Piga N, Chapon F, Godfrain C, Tournier-Lasserre E. The ectodomain of the Notch3 receptor accumulates within the cerebrovasculature of CADASIL patients. *J Clin Invest.* 2000;105:597–605.
9. Joutel A, Vahedi K, Corpechot C, Troesch A, Chabriat H, Vayssiere C, Cruaud C, Maciazek J, Weissenbach J, Bousser MG, Bach JF, Tournier-Lasserre E. Strong clustering and stereotyped nature of Notch3 mutations in CADASIL patients. *Lancet.* 1997;350:1511–1515.
10. Baudrimont M, Dubas F, Joutel A, Tournier-Lasserre E, Bousser M. Autosomal dominant leukoencephalopathy and subcortical ischemic strokes: a clinicopathological study. *Stroke.* 1993;24:122–125.
11. Ruchoux MM, Maurage CA. CADASIL: cerebral autosomal dominant arteriopathy with subcortical infarcts and leukoencephalopathy. *J Neuro-pathol Exp Neurol.* 1997;56:947–964.

12. Chabriat H, Levy C, Taillia H, Iba-Zizen MT, Vahedi K, Joutel A, Tournier-Lasserre E, Bousser MG. Patterns of MRI lesions in CADASIL. *Neurology*. 1998;51:452-457.
13. Yousry TA, Seelos K, Mayer M, Bruning R, Uttner I, Dichgans M, Mammi S, Straube A, Mai N, Filippi M. Characteristic MR lesion pattern and correlation of T1 and T2 lesion volume with neurologic and neuropsychological findings in cerebral autosomal dominant arteriopathy with subcortical infarcts and leukoencephalopathy (CADASIL). *AJNR Am J Neuroradiol*. 1999;20:91-100.
14. Dichgans M, Filippi M, Brüning R, Iannucci G, Berchtenbreiter C, Minicucci L, Uttner I, Crispin A, Ludwig H, Gasser T, Yousry T. Quantitative MRI in CADASIL. *Neurology*. 1999;52:1361-1367.
15. Le Bihan D, Breton E, Lallemand D, Grenier P, Cabanis E, Laval-Jeantet M. MR imaging of intravoxel incoherent motions: application to diffusion and perfusion in neurologic disorders. *Radiology*. 1986;161:401-407.
16. Le Bihan D, Mangin JF, Poupon C, Clark CA, Pappata S, Molko N, Chabriat H. Diffusion tensor imaging: concepts and applications. *J Magn Reson Imaging*. 2001;13:534-546.
17. Pierpaoli C, Jezzard P, Basser PJ, Barnett A, Di Chiro G. Diffusion tensor MR imaging of the human brain. *Radiology*. 1996;201:637-648.
18. Filippi M, Cercignani M, Inglese M, Horsfield MA, Comi G. Diffusion tensor magnetic resonance imaging in multiple sclerosis. *Neurology*. 2001;56:304-311.
19. Rose SE, Chen F, Chalk JB, Zelaya FO, Strugnell WE, Benson M, Semple J, Doddrell DM. Loss of connectivity in Alzheimer's disease: an evaluation of white matter tract integrity with colour coded MR diffusion tensor imaging. *J Neurol Neurosurg Psychiatry*. 2000;69:528-530.
20. Agartz I, Andersson JL, Skare S. Abnormal brain white matter in schizophrenia: a diffusion tensor imaging study. *Neuroreport*. 2001;12:2251-2254.
21. Klingberg T, Hedehus M, Temple E, Salz T, Gabrieli JD, Moseley ME, Poldrack RA. Microstructure of temporo-parietal white matter as a basis for reading ability: evidence from diffusion tensor magnetic resonance imaging. *Neuron*. 2000;25:493-500.
22. Chabriat H, Pappata S, Poupon C, Clark C, Vahedi K, Poupon F, Mangin J, Pachot-Clouard M, Jobert A, Le Bihan D, Bousser M. Clinical severity in CADASIL related to ultrastructural damage in white matter: in-vivo study with diffusion tensor MRI. *Stroke*. 1999;30:2637-2643.
23. Molko N, Pappata S, Mangin JF, Poupon C, Vahedi K, Jobert A, LeBihan D, Bousser MG, Chabriat H. Diffusion tensor imaging study of subcortical gray matter in CADASIL. *Stroke*. 2001;32:2049-2054.
24. MacKenzie DM, Copp P, Shaw RJ, Goodwin GM. Brief cognitive screening of the elderly: a comparison of the Mini-Mental State Examination (MMSE), Abbreviated Mental Test (AMT) and Mental Status Questionnaire (MSQ). *Psychol Med*. 1996;26:427-430.
25. Cockrell JR, Folstein MF. Mini-Mental State Examination (MMSE). *Psychopharmacol Bull*. 1988;24:689-692.
26. American Psychiatric Association. *Diagnostic and Statistical Manual of Mental Disorders, Third Edition*. Washington, DC: American Psychiatric Association; 1987.
27. Rankin J. Cerebral vascular accidents in patients over the age of 60. *Scott Med J*. 1957;2:210-215.
28. De Haan R, Limburg M, Bossuyt P, Van der Meulen J, Aaronson N. The clinical meaning of Rankin "handicap" grades after stroke. *Stroke*. 1995;26:2027-2030.
29. Poupon C, Clark CA, Frouin V, Regis J, Bloch I, Le Bihan D, Mangin J. Regularization of diffusion-based direction maps for the tracking of brain white matter fascicles. *Neuroimage*. 2000;12:184-195.
30. Basser P, Mattiello J, Le Bihan D. Estimation of the effective self-diffusion-tensor from the NMR spin echo. *J Magn Reson*. 1994;103:247-254.
31. van Buchem MA, McGowan JC, Kolson DL, Polansky M, Grossman RI. Quantitative volumetric magnetization transfer analysis in multiple sclerosis: estimation of macroscopic and microscopic disease burden. *Magn Reson Med*. 1996;36:632-636.
32. Rovaris M, Filippi M, Calori G, Rodegher M, Campi A, Colombo B, Comi G. Intra-observer reproducibility in measuring new putative MR markers of demyelination and axonal loss in multiple sclerosis: a comparison with conventional T2-weighted images. *J Neurol*. 1997;244:266-270.
33. Sormani MP, Iannucci G, Rocca MA, Mastronardo G, Cercignani M, Minicucci L, Filippi M. Reproducibility of magnetization transfer ratio histogram-derived measures of the brain in healthy volunteers. *AJNR Am J Neuroradiol*. 2000;21:133-136.
34. Iannucci G, Dichgans M, Rovaris M, Bruning R, Gasser T, Giacomotti L, Yousry TA, Filippi M. Correlations between clinical findings and magnetization transfer imaging metrics of tissue damage in individuals with cerebral autosomal dominant arteriopathy with subcortical infarcts and leukoencephalopathy. *Stroke*. 2001;32:643-648.